

1
2
3 1
4 2
5 3
6 4
7 5
8 6
9 7
10 8
11 9
12 10
13 11
14 12
15 13
16 14
17 15
18 16
19 17
20 18
21 19
22 20
23 21
24 22
25 23
26 24
27 25
28 26
29 27
30 28
31 29
32 30
33 31
34 32
35
36
37
38
39
40
41
42
43
44
45
46
47
48
49
50
51
52
53
54
55
56
57
58
59
60

Disentangling the population structure and evolution of the clam pathogen *Vibrio tapetis*.

Sabela Balboa, Asmine Bastardo, Jesús L. Romalde*

Departamento de Microbiología y Parasitología. CIBUS-Facultad de Biología.
Universidad de Santiago de Compostela. 15782, Santiago de Compostela. Spain.

Running title: Population structure and evolution of *V. tapetis*.

Key words: *Vibrio tapetis*, MLST, population, evolution.

Submitted to: **FEMS Microbiology Ecology**, February 2013.

* Jesús L. Romalde. Departamento de Microbiología y Parasitología. CIBUS-Facultad de Biología. Campus vida. Universidad de Santiago de Compostela. C/ Lope Gómez de Marzoa s/n. 15782, Santiago de Compostela. Spain. Phone: +34 881816908. Fax: +34 881896938. E-mail: jesus.romalde@usc.es

33 **SUMMARY**

34

35 *Vibrio tapetis* is a fastidious slow-growing microorganism that causes the Brown Ring
36 Disease (BRD) in clams. Recently, two subspecies for this bacterial pathogen have been
37 proposed. We have developed a MSLT scheme and performed evolutionary studies of
38 *V. tapetis* population using the great majority of isolates of *V. tapetis* obtained
39 worldwide until now (30 isolates). *V. tapetis* constitutes a high polymorphic population,
40 showing low diversity indexes and some genetic discontinuity among the isolates.
41 Mutation events are more frequent than recombination, although both are approximately
42 equally important for genetic diversification. In fact, the divergence between subspecies
43 occurred exclusively by mutation but the diversity observed among isolates of the same
44 subspecies appeared to be generated mostly by recombination. Between the subspecies,
45 genetic distance is very high and almost no recurrent gene flow exists. This pathogen
46 displays a non-clonal population structure with an ancient spatial segregation population
47 and some degree of geographical isolament, followed by a population expansion, at
48 least for *V. tapetis* subsp. *tapetis*. A database from this study was created and hosted on
49 pubmlst.org, being freely available (<http://pubmlst.org/vtapetis/>).

50

51

52

53 INTRODUCTION

54 A population is defined as an assemblage of individuals of the same species in a more
55 or less geographically restricted area (Hanage *et al.*, 2006; Sikorski, 2008). The
56 evolutionary fate of a population is defined by mutation, recombination, natural
57 selection and genetic drift. Combinations of these interactions can be schematically
58 assigned to different evolutionary models (Cohan & Perry, 2007). Recombination
59 and/or mutation play a major role in determining genetic variability and establishing
60 different ways of species evolution (i.e., diversifying, directional, purifying). Therefore,
61 their study is a fundamental prerequisite for better understanding the epidemiology and
62 the disease cycle of a pathogen. On the other hand, dispersal, geographic isolation, past
63 range restrictions and expansions, drift processes, founder events and selection leave
64 their signature in the lineage composition of contemporary populations (Avisé, 2000).

65 Multilocus Sequence Typing (MLST) is a powerful technique for inferring the genetic
66 relationships among bacteria, at both interspecific and intraspecific levels, by using core
67 housekeeping genes (Maiden, 2006). This technique was successfully applied for many
68 pathogenic and commensal bacterial species, and is currently regarded as the gold-
69 standard in molecular typing being able to even replace Pulsed Field Gel
70 Electrophoresis (PFGE) and Multilocus Enzyme Electrophoresis (MLEE) (Maiden,
71 2006). Moreover, when coupled with the appropriate statistical tests and algorithms, it
72 can help to unravel evolutionary dynamics (i.e., population evolution).

73 *Vibrio tapetis* is the causative agent of Brown Ring Disease (BRD) in adult clams. The
74 disease has been detected for years in Europe and, more recently, in Asia. Some typing
75 studies have been carried out for this species. At genetic level, differences were first
76 detected in the plasmid content and ribotypes of the strains (Paillard, 2004; Borrego *et al.*,
77 2011). Subsequently, on the basis of studies with PCR-based typing techniques,
78 three major groups associated with the host origin were established (Rodríguez *et al.*,
79 2006). More recently, our group has carried out a MLSA study and described a new
80 subspecies for this pathogen, *V. tapetis* subsp. *britannicus* (Balboa & Romalde, 2013).

81 In this work, we have developed a MLST scheme and performed evolutionary studies
82 on the population of *V. tapetis*, including both subspecies, to achieve a better knowledge
83 of the distribution and the evolution of this pathogen.

84

85

86

87 MATERIALS AND METHODS

88

89 Bacterial Strains

90 A total of 30 strains of *V. tapetis* were used in this study (Table 1). These isolates were
91 obtained from different hosts and were temporal and geographically diverse. To our
92 knowledge, they constitute the great majority of *V. tapetis* strains isolated until now
93 worldwide. The collection includes strains belonging to the two subspecies and
94 representatives for the three genetic groups previously described for the species
95 (Rodríguez *et al.*, 2006; Balboa & Romalde, 2013). Bacteria were routinely grown on
96 marine agar (MA, Pronadisa) and incubated at 15°C for 72h.

97

98 DNA Purification and Gene Amplification and Sequencing

99 Chromosomal DNA was extracted from pure bacterial cultures using the Insta-Gene
100 matrix (Bio-Rad, Madrid, Spain) as previously described by Romalde *et al.* (1999). Ten
101 gene loci were selected for MLST analysis, including (*atpA* (α subunit of ATPase), *fstZ*
102 (cell division protein), *gapA* (glyceraldehydes-3-phosphodehydrogenase), *hsp60*, (60-
103 KDs heat shock protein), *pyrH* (uridyl monophosphate kinase), *rctB* (Replication
104 origin-binding protein), *recA* (recombinase A), *rpoA* (α subunit of RNA polymerase)
105 and *rpoD* (RNA polymerase sigma factor), *topA* (topoisomerase I). PCR conditions and
106 primer sequence are described in <http://pubmlst.org/vtapetis/>.

107 DNA sequences were performed as described Balboa & Romalde (2013). Briefly,
108 amplified fragments were sequenced in both directions using GenomeLab DTCS-Quick
109 Start Kit (Beckman Coulter, Ireland) in a Beckman coulter sequencer (Beckman
110 Coulter, Ireland). *fstZ* and *rpoD* sequences were performed at Stabvida Lcd. (Portugal).
111 Sequence data analysis was performed with DNASTar Seqman program (Lasergene,
112 USA) and the DNA sequences were aligned and translated into amino acid sequences
113 using the MEGA5 software (Tamura *et al.*, 2011).

114

115 Genetic Analysis of the Population

116 According to MLST standard (Urwin & Maiden, 2003), a distinct ST number was
117 attributed to each distinct profile of alleles types (ATs; particular alleles at particular
118 loci).

119 A descriptive analysis of nucleotide and allele diversity was performed for the
120 individual genes and the concatenated sequence (5826 bp in length). Thus, the average

1
2
3 121 gene diversity was calculated using Nei's index of diversity (H) (Nei, 1978) and the
4 122 type of selection was determined by the ratio of mean non-synonymous substitutions
5 123 per non-synonymous site/mean synonymous substitution per synonymous site (d_N/d_S
6 124 ratio) according to Nei and Gojobori (Nei & Gojobori, 1986) method with the Jukes-
7
8
9 125 Cantor correction.

10
11 126 Number of polymorphic sites and the index of association (I_A) was performed using the
12 127 START2 program (<http://pubmlst.org/software/analysis/start2/>). The "standardized"
13 128 index of association (I_A^S) from the allelic profile dataset of the whole collection as well
14
15 129 as for the STs defined in the study were calculated (Maynard-Smith *et al.*, 1993).
16
17
18 130

19 131 **Population Structure**

20
21 132 The clonal structure of the population was determined using eBURST v3.0 program
22 133 <http://eburst.mlst.net>. On a different approach, a dot graph was constructed using a 50%
23 134 majority rule consensus tree was done using ClonalFrame version 1.1 (Didelot &
24 135 Falush, 2007) using 10 independent runs of MCMC (Markov Chain Monte Carlo). On
25
26 136 the other hand, a phylogenetic reconstruction was performed for the whole collection of
27
28 137 isolates by Neighbour joining method, using Kimura-2-parameters method and
29 138 bootstrap of 1,000 replicates, with MEGA5 program (Tamura *et al.*, 2001).
30
31
32

33 139 The relationships among haplotypes were displayed in a network constructed by Median
34 140 Joining method using the programs DNA Alignment 1.3 and NETWORK 4.1 (Fluxus-
35 141 engineering) (Bandelt *et al.*, 1999).
36
37
38 142

39 143 **Recombination**

40
41 144 Putative recombination events were detected using three different approaches. The
42 145 minimal number of recombination events R_{\min} was computed on biallelic site only by
43 146 using DnaSP5 software (Librado & Rozas, 2009). The identification of recombination
44 147 sequences and breakpoints were identified using RDP4 Beta (Martin *et al.*, 2010).
45
46 148 Finally, SplitsTree versión 4.0 (Huson & Bryant, 2006) was employed to calculate the
47 149 phi test for recombination for the whole strain collection, and to generate a Split-tree for
48
49 150 each individual locus as well as for the concatenated sequence.
50
51
52

53 151 54 152 **Clonal Genealogy**

55
56 153 The clonal genealogy of the whole population was inferred with ClonalFrame (Didelot
57 154 & Falush, 2007) using 100000 MCMC. Mixing and convergence properties were found
58
59
60

1
2
3 155 to be satisfactory based on comparisons of independent runs. For presentation purposes,
4 156 the estimated genealogies were represented in a 50% majority rule consensus tree.
5
6
7

8 158 **Demographic History and Gene Flow**

9
10 159 The average number of nucleotides per site (π) and the number of segregating sites (θ)
11 160 were computed using both DnaSP5 (Librado & Rozas, 2009) and Arlequin v3.5
12 161 (Excoffier & Lischer, 2010) programs that were also employed to calculate the values
13 162 of selection tests based on polymorphism distribution. The tests of Tajima (Tajima,
14 163 1989) and Fu and Li (Fu & Li, 1993) F^* and D^* were used to confirm the hypothesis
15 164 that all mutations are selectively neutral (Kimura, 1983).

16 165 Fu's F_S (Fu, 1997) and Strobeck's S (Strobeck, 1987) statistics were calculated to assess
17 166 the haplotype structure based on the haplotype frequency distribution. The later is also
18 167 considered as an index of admixture, characteristic of populations originated from
19 168 multiple sources. Onsis R_2 -test is based on the difference between the number of
20 169 singleton mutations in a population and the average number of nucleotide differences in
21 170 that population, with lower values of the statistics expected after a recent episode of
22 171 severe population growth (Ramos-Onsins & Rozas, 2002).

23 172 The gene flow between the two subspecies was assessed by the fixation index (F_{ST}),
24 173 which measures the differentiation among individuals within population (Wright, 1951).
25 174 Nei's G_{ST} , to analyze the population differentiation based on differences in allele
26 175 frequencies, and N_M , to estimate gene flow on the basis of G_{ST} (Nei, 1978), were
27 176 calculated with the Arlequin v3.5 software. To estimate the correlation between genetic
28 177 (determined using F_{ST}) and geographical distances, a Isolation By Distance (IBD) test
29 178 was performed using the program IBDWS (Jensen *et al.*, 2005). Non-parametric Mantel
30 179 test was carried out with the full dataset to analyse non-random associations between
31 180 genetic and geographical distances. Genetic distances were computed using Slatkin's
32 181 (Slatkin, 1993) similarity measure: $M = ([1/F_{ST}] - 1)/4$. The significance of the Mantel
33 182 test was determined by a permutation test of $n=1000$. Isolates were grouped in four
34 183 groups according to their country of origin. Geographical distances were measured
35 184 using geographical coordinates.

36 185 The software packages DnaSP5 and Arlequin v3.5 were also used to calculate frequency
37 186 distributions of number of mismatches between pairwise sequences, and to model the
38 187 expected distributions under the demographic scenarios of constant and decline growth
39 188 of population size, population expansion and spatial expansion. Model fitness was
40
41
42
43
44
45
46
47
48
49
50
51
52
53
54
55
56
57
58
59
60

1
2
3 189 examined by raggedness r statistic, which indicates the smoothness of the mismatch
4 190 distribution (Rogers and Harpending, 1992).

5
6 191

7 8 192 **RESULTS**

9 193

10 194 **Nucleotide Diversity**

11 195 A total of 5,826 bp at 10 loci were sequenced from 30 strains of *V. tapetis* (Table 1).
12 196 The in-frame DNA fragments ranged in size from 516 bp (*pyrH*) to 609 bp (*fstZ*)
13 197 (<http://pubmlst.org/vtapetis/>). A descriptive analysis of nucleotide and allele diversity is
14 198 shown in Table 2. Four hundred and fifty polymorphic sites were recorded, being only 8
15 199 of them (located in genes *fstZ*, *gapA*, *hsp60*, *rctB* and *recA*) triallelic. The locus with
16 200 more polymorphic sites was *rctB* (93 biallelic and 2 triallelic sites), in contrast with
17 201 *rpoA* in where only 7 sites were found polymorphic, being all of them biallelic. The
18 202 number of alleles observed for each locus varied from 3 (*rpoA*) to 9 (*recA* and *topA*),
19 203 being identified a total of 72 different alleles, 34 of which were synapomorphic (i.e.
20 204 shared and derived). The most frequently found allele was allele 1 in all loci analyzed,
21 205 with percentages ranging from 56.7% for *rctB*, *recA*, *rpoD* and *topA* and 80% for *fstZ*.
22 206 The most polymorphic loci were *recA* and *topA* that showed 9 different alleles,
23 207 although those genes, together with *atpA*, *gapA*, *pyrH* and *rpoD* retained more
24 208 synapomorphic alleles. When the 72 alleles were combined for the 30 isolates of *V.*
25 209 *tapetis*, a total of 10 sequence types (STs) could be identified (Table 1), indicating high
26 210 diversity in the population.

27 211 The number of polymorphic sites was overall low and found to be 7.7% for the
28 212 concatenated sequences. The average number of nucleotides per site (π) and the number
29 213 of segregating sites (θ) were 0.015 and 0.020, respectively. Values of π and θ for each
30 214 individual gene in the whole population and in each subspecies are shown in Tables 2
31 215 and S1.

32 216 Values of test for selection (d_N/d_S ratio) calculated for the concatenated sequence and
33 217 for each individual locus were <1 (in particular *gapA* gave a $d_N/d_S = 0$), indicating that
34 218 all these loci were subjected to positive selection, i.e., under stabilizing or purifying
35 219 selection.

36 220 Linkage disequilibrium was estimated with the I_A parameter from allelic profiles with
37 221 randomized data sets, rendering values of 6.300 ($P = 0.000$), for whole strain collection,
38 222 and 1.584 ($P = 0.000$) when only the STs were analyzed. Standardized I_A^S values,

1
2
3 223 calculated to avoid dependence on the number of loci, were lower, 0.700 ($P =$
4 224 0.000)(whole strain collection) and 0.176 ($P = 0.000$) (STs), but still significantly
5
6 225 different from zero. Similar results were obtained *V. tapetis* subsp. *tapetis*, $I^S_A = 0.649$
7
8 226 ($P = 0.000$) analysing all the isolates, and $I^S_A = 0.111$ ($P = 0.000$) obtained in the STs
9
10 227 analysis. Hence, a non-random distribution of alleles in the *V. tapetis* population was
11
12 228 observed, although some recombination may also occur.
13

229

230 **Population Structure**

16 231 Seven STs were represented by a single isolate, while the other three included 2, 4 and
17
18 232 17 isolates. It was not possible to identify any clonal complexes by eBURST with the
19
20 233 most stringent criteria (9/10 shared alleles). Thus, all STs were considered as singletons
21
22 234 with no apparent clonal relationship to each other, which probably reflects some genetic
23
24 235 discontinuity among the strains (Fig. S1A). When the strains were visualized in a dot
25
26 236 graph constructed using a 50% majority rule consensus tree (Fig. S1B), some missing
27
28 237 intermediates showed up and the existence of some putative clonal complexes was
29
30 238 evidenced. Therefore, *V. tapetis* population displays a level of genetic structure that
31
32 239 cannot be detected using conventional MLST. The existence of these intermediates was
33
34 240 also evident in the network constructed by Median Joining algorithm where these
35
36 241 putative variants constituted the linkage among the established STs (Fig. 1).

37
38 242 To explore the phylogenetic relationships among 30 *V. tapetis* isolates, a phylogenetic
39
40 243 tree was performed using the Neighbor joining (NJ) algorithm. This tree shows two
41
42 244 clearly differentiated clusters (Fig S2), each corresponding with one subspecies.

245

246 **Recombination**

43 247 The phi test (Pairwise Homoplasy Test) did not indicated significant statistical
44
45 248 evidences for recombination in any gene or the concatenated sequences. However, some
46
47 249 putative recombination events were detected with the minimal number of recombination
48
49 250 events R_{\min} . Specifically, one event of recombination was found in *atpA*, *pyrH* and
50
51 251 *rctB*, four events were found in *recA* and five in *rpoD*. Using RDP4 software, five
52
53 252 events of recombination were found in *atpA* and one in *fstZ*.

54 253 The split graph based on the concatenated sequences displayed an interconnecting
55
56 254 network structure rather than a single bifurcation tree (Fig. 2). This structure indicates
57
58 255 the presence of homoplasies (repeated mutations at the same nucleotide sites at
59
60 256 independent links of a phylogenetic tree) that are most probably a result from intragenic

1
2
3 257 recombination. The network structures of those genes showing recombination can be
4
5 258 also seen in the splits graphs constructed for each individual gene (Fig S3).
6
7 259 ClonalFrame analyses estimated that mutation was considerably more frequent than
8
9 260 recombination within this dataset ($\rho/\theta = 0.084$, 95% CI: 0.045-0.183) but they were
10
11 261 approximately equally important for genetic diversification ($r/m = 1.470$, 95% CI:
12
13 262 0.842-2.724). The clonal genealogy confirmed the mutational character of the
14
15 263 divergence between subspecies (Fig. 3). Sequence variations on the oldest branch of the
16
17 264 tree (node A) seems to arise exclusively by mutational events while in the younger
18
19 265 branches recombination imports are common although mutational events are also
20
21 266 present. It is noteworthy that intermediate-evolutive branches (nodes B and H) are the
22
23 267 ones that showed more recombinatorial events, suggesting that the diversity within each
24
25 268 subspecies was mostly generated by recombination.

269 270 **Gene Flow**

271 Isolates from the two subspecies differed between 6.8 and 7.1% in the concatenated
272
273 sequence. These nucleotide differences were accompanied by high population specific
274
275 fixation index values ($F_{ST} = 0.952$, $P = 0$). Such a value, together with a $G_{ST} = 0.105$
276
277 illustrates in full view the magnitude of the separation of those groups of isolates.
278
279 Moreover, a N_M of 0.07 indicates that the genetic exchange between both groups is
280
281 almost non-existent.

282 283 **Demographic Trends**

284 All the statistics and site frequent spectra analysed were consistent with a deviation
285
286 from the neutral mode, although some incongruences among the different indexes were
287
288 observed (Table 3). Tajima's D showed negative although non-significant value,
289
290 reflecting an excess of rare polymorphisms in the population, which is consistent with
291
292 either positive selection or an increase in population size. On the contrary, Fu and Li F^*
293
294 and D^* showed positive, and most of them, non-significant values reflecting an excess
295
296 of intermediate-frequency alleles in the population that can be the result of either
297
298 balancing selection or population bottleneck (i.e. population subdivision). The positive
299
300 values of Fu's F_S constituted an evidence for a deficiency of alleles, as would be
301
302 expected from a recent population bottleneck or from overdominant selection. Onis R_2
303
304 values close to zero supported the population expansion pattern, while Strobeck's S'
305
306 statistic indicated the non-admixture of the population.

1
2
3 291 Regarding to the subpopulations, the indexes were calculated only for *V. tapetis* subsp.
4 292 *tapetis* that showed evidences for positive selection or an increase in population size
5 293 regardless the index employed, as well as evidences for admixture in the population
6 294 (Table S2).

7
8
9 295 It is noteworthy that some genes, namely *atpA* and *fstZ*, showed a deviation for the
10 296 general trend of the population. The same was observed for *atpA*, *rctB* and *rpoD* genes
11 297 in the subspecies *tapetis*.

12 298 The mismatch distribution was not significantly different from those expected under
13 299 either spatial expansion or population size expansion models (Fig. 4). The observed
14 300 mismatch distribution was multimodal and showed four distinct peaks. The distribution
15 301 fitted with the expected model for spatial expansion, although Harpending's raggedness
16 302 index ($r = 0.176$) was only significant under a population expansion model ($P = 0.01$).
17 303 When the pairwise mismatch distributions were calculated for *V. tapetis* subsp. *tapetis*
18 304 evidence for population expansion was apparent ($r = 0.086$, $P = 0.5$).

19 305 The spatial structure of allele frequencies was assessed using Moran's I statistic, a
20 306 coefficient of spatial dependence for pairs of samples separated into distance classes
21 307 according to their country of origin (4 distance classes). The resulting correlogram of
22 308 spatial dependence (Fig. 5) revealed that the spatial correlation decreased with
23 309 increasing pairwise distances, being in addition lower than it would be expected in a
24 310 random dataset at two of the larger distance classes. This finding indicates that allele
25 311 frequencies in neighbouring sites tend to be more similar when they are geographically
26 312 closer. Nonetheless, the Mantel test (M), for correlation between genetic similarity and
27 313 geographic distance using the shortest distance over land, showed non-significant
28 314 negative correlation for the full dataset ($Z = 4463.971$, $r = 0.180$, $P = 0.657$).

29 315

30 316 **DISCUSSION**

31 317 The MLST approach of this study was motivated by a previous phylogenetic work
32 318 performed by our group using, to our knowledge, the great majority of isolates of *V.*
33 319 *tapetis* obtained worldwide until now (Balboa & Romalde, 2013). This study led to the
34 320 description of two subspecies for *V. tapetis* associated to the geographical origin of the
35 321 isolates. Thus, the subspecies *britannicus* is restricted to the British Isles, while
36 322 subspecies *tapetis* comprises isolates from all other locations. The variability within
37 323 each subspecies is associated to host origin, in agreement with the results previously
38 324 obtained by Rodríguez *et al.* (2006). In this work, we tried to shed light on the
39
40
41
42
43
44
45
46
47
48
49
50
51
52
53
54
55
56
57
58
59
60

1
2
3 325 emergence and evolution of *V. tapetis* since its genetic structure is very intriguing,
4 326 showing high heterogeneity with genetic discontinuity.
5
6 327 The first obvious achievement was the polymorphism found among the isolates. Thus,
7
8 328 and having in mind the scarce number of isolates, a total of 450 polymorphic sites were
9
10 329 described among the 5826 bp. Despite this fact, the nucleotide diversity per site (π) and
11
12 330 the average number of nucleotide differences per site (θ) indicated a relative low degree
13
14 331 of sequence diversity. This fact has been partially attributed in other aquatic bacterial
15
16 332 pathogens to the selection of particular strains in the collection (Yan *et al.*, 2011;
17
18 333 Bastardo *et al.*, 2012), as occur in this case where ST1 is formed by 17 strains while
19
20 334 most of STs are constituted by a single isolate. On the other hand, the average of π in
21
22 335 each subspecies is ten-fold lower than in the species as a whole, suggesting that barriers
23
24 336 to genetic exchange between subspecies could be formed in a DNA sequence
25
26 337 homology-dependent manner (Tanabe & Watanabe, 2011). Only 51 out of the 450
27
28 338 polymorphic sites corresponded to non-synonymous changes, consistent with a strong
29
30 339 selection against amino acid changes, as typically observed for housekeeping genes
31
32 340 (Pérez-Losada *et al.*, 2006).

33
34 341 The lack of clonal complexes reflected some genetic discontinuity among the strains,
35
36 342 but it has been demonstrated that the eBURST can only identify recent divergence of
37
38 343 clones on the basis of shared allele at multiple loci. Therefore, it can produce
39
40 344 incongruent results if the role of recombination has increased in recent times (Feil *et al.*,
41
42 345 2004). The dot graph generated by ClonalFrame confirmed the existence of missing
43
44 346 intermediates in the population, suggesting that the two subspecies diverged in a long-
45
46 347 term evolutionary consequence rather than a recent diversification. On the other hand, it
47
48 348 is important to emphasize at this point that the small amount of isolates belonging to
49
50 349 this species may be distorting the structure of the population. The lack of isolates can be
51
52 350 probably related to the fact that *V. tapetis* is a slow-growing difficult-to-isolate pathogen
53
54 351 (Balboa *et al.*, 2012) that most of times, even when is detected by indirect procedures
55
56 352 such as PCR, it cannot be recovered on culture media (Drummond *et al.*, 2007; Paillard,
57
58 353 2004; Borrego *et al.*, 2011).

59
60 354 The differentiation between subspecies together with the lack of clonal relationships
61
62 355 exhibited by the STs could lead to think that they are two different species. However,
63
64 356 the NJ tree supported a high phylogenetic relationship, showing all branches more than
65
66 357 87% bootstrap. In addition, our previous study of MLSA demonstrated a clear
67
68 358 monophyletic nature of *V. tapetis* as bacterial species and further DDH experiments

1
2
3 359 confirmed that the three isolates of *V. tapetis* subsp. *britannicus* belong indeed to *V.*
4 360 *tapetis* species (Balboa & Romalde, 2013).

5
6 361 Mutation and recombination are equally important for genetic diversification of *V.*
7 362 *tapetis*. As it was demonstrated with the clonal genealogy, the separation of the two
8 363 subspecies occurred exclusively by mutation, and these mutational events were
9 364 quantified in 370 with the construction of the median joining network. Such amount of
10 365 mutational events together with the differences between the I_A^S values for the whole
11 366 population and for STs, indicate that although recombination occurs at a considerably
12 367 frequency, it is not enough for allele random association (de las Rivas *et al.*, 2006). On
13 368 the other hand, the amount of recombination showed by Clonal genealogy could not be
14 369 demonstrated using other methods such as phi test, which can be probably due to the
15 370 fact that the genes used in this study are under purifying selection, purging any
16 371 sequence variation required for the detection of intragenic recombination by most
17 372 algorithms (Feil *et al.*, 2004)

18 373 Despite the limited sequence diversity evidenced by the low π and θ values, the majority
19 374 of STs occurred as singletons, which suggests that the sequence diversity was magnified
20 375 by extensive intraspecies recombination, generating genotypes which can be readily
21 376 distinguished by sequence analysis (Brisse *et al.*, 2009).

22 377 The existence of the high genetic distance between the two subspecies is confirmed by
23 378 F_{ST} and G_{ST} indexes and little or no recurrent gene flow ($Nm < 1$), explaining the lack of
24 379 recombinational events among strains of the two different subspecies. Such a genetic
25 380 distance may be the result of vicariance or obstruction by natural barriers but, although
26 381 the inference of range expansion was well supported by Moran's index, the isolation by
27 382 distance (IBD) was not significant.

28 383 Despite the high I_A^S showed by the entire population, the lack of IBD together with the
29 384 low nucleotide diversity and the frequent recombination among strains within each
30 385 subspecies evidence a non-clonal population structure for *V. tapetis*. Moreover, the
31 386 appearance of the dominant ST1 that, together with ST2, are the only STs of
32 387 demonstrated pathogenicity (Paillard, 2004) reminds to the emergence of highly
33 388 adaptive bacterial clones in epidemic populations, where a small number of successful
34 389 clones dramatically increase their population size with respect to the other genotypes
35 390 (Smith *et al.*, 1993).

36 391 The frequency distribution of pairwise mismatches of neutral-evolving loci showed
37 392 multimodal distribution with high degree of raggedness, as expected for a population in

1
2
3 393 constant expansion (Slatkin & Hudson, 1991; Rogers & Harpending, 1992; Ray *et al.*,
4 394 2003). Tajima's D^* and Onsis R_2 (Tajima, 1989; Ramos-Onsis & Rozas, 2002) values
5 395 confirmed the evidences for population expansion while F_S (Fu, 1997) indicates
6 396 that the population suffered a bottleneck, for example a subdivision of the population.
7
8 397 Although it is well known that F_S is a more sensitive indicator for population expansion
9 398 and genetic hitchhiking than D^* , it has also been described that the former statistic is
10 399 highly affected by recombinational events (Fu, 1997). However, the powerful Onsis R_2
11 400 test, which is particularly suited for small size samples with recombination, also
12 401 supports the population expansion detected by the mismatch distribution. This apparent
13 402 contradiction may be explained by the lower statistical power of these tests compared to
14 403 mismatch distribution to detect spatial expansions when local demes exchange only few
15 404 migrants (Ray *et al.*, 2003; Städler *et al.*, 2009). F^* and D^* values are positive,
16 405 indicating a deficit of mutation in the external branches. This statistic reflects an
17 406 unusually amount of ancient alleles probably maintained by balancing selection.
18 407 Nonetheless, it is impossible to distinguish between selection and expansion as the
19 408 cause of negative F_S , D^* and F^* values. It is noteworthy that some genes showed a
20 409 deviation from the general trend of the population, being indicative of selective
21 410 pressures unique to one population (i.e., local adaptation), different demographic
22 411 histories, spurious results, or most likely some complex combination of all of these
23 412 factors. The evidences for admixture found in *V. tapetis* subsp. *tapetis* population are
24 413 probably a result of the introduction of new genetic lineages into the population.
25 414 These statistics in combination with mismatch distribution indicate an ancient spatial
26 415 segregation of the population with some degree of geographical isolation, that probably
27 416 caused the apparition of the two subspecies, followed by a population expansion, at
28 417 least for *V. tapetis* subsp. *tapetis*.
29 418 A database from this study was created and hosted on pubmlst.org (Jolley & Maiden,
30 419 2010) and is freely available in Internet (<http://pubmlst.org/vtapetis/>). This database will
31 420 be useful in future works studying evolutionary and epidemiological relationships
32 421 between strains and for unambiguous comparison of data generate from laboratories
33 422 around the world.
34
35
36
37
38
39
40
41
42
43
44
45
46
47
48
49
50
51
52
53
54
55
56
57
58
59
60

1
2
3 425

4 426 **Acknowledgements**

5
6 427 This work was supported in part by grant AGL2010-18438 from the Ministerio de
7
8 428 Ciencia e Innovación (Spain). S.B. acknowledges the Ministerio de Ciencia e
9
10 429 Innovación (Spain) for a research fellowship.

11 430 The authors have no conflict of interest to declare.

12
13 431

14 432

15 433

16 434

17 435

18 436

19 437

20 438

21 439

22 440

23
24
25
26
27
28
29
30
31
32
33
34
35
36
37
38
39
40
41
42
43
44
45
46
47
48
49
50
51
52
53
54
55
56
57
58
59
60

For Peer Review

441 **REFERENCES**

- 442
- 443 Avise JC (2000) Phylogeography: the history and formation of species. Harvard
444 University Press, Harvard.
- 445 Balboa S & Romalde JL (2013) Multilocus sequence analysis of *Vibrio tapetis*, the
446 causative agent of Brown Ring Disease. Description of *Vibrio tapetis* subsp.
447 *britannicus* subsp. nov. *Syst Appl Microbiol* doi: 10.1016/j.syapm.2012.12.004.
- 448 Balboa S, Dieguez, AL, Doce A, Barja JL & Romalde JL (2012) Evaluation of different
449 culture media for the isolation and growth of the fastidious *Vibrio tapetis*, the
450 causative agent of brown ring disease. *J Invertebr Pathol* 111: 74-81.
- 451 Bandelt HJ, Fortser P & Röhl A (1999) Median-joining networks for inferring
452 intraspecific phylogenies. *Mol Biol Evol* 16: 37-48.
- 453 Bastardo A, Ravelo C & Romalde JL (2012) Multilocus sequence typing reveals high
454 genetic diversity and epidemic population structure for the fish pathogen *Yersinia*
455 *ruckeri*. *Environ Microbiol* 14: 1888-97.
- 456 Borrego JJ, Romalde JL & Castro D (2011) La enfermedad del anillo marrón. In
457 *Enfermedades de moluscos bivalvos de interés en acuicultura*. (Figueras A & Novoa
458 B, eds) pp 149-179. Fundación OESA.
- 459 Brisse F, Fevre C, Passet V, Issenhuth-Jeanjean S, Tournebize R, Diancourt L &
460 Grimont P (2009) Virulent clones of *Klebsiella pneumoniae*: identification and
461 evolutionary scenario based on genomic and phenotypic characterization. *PLoS One*
462 4: e4982.
- 463 Cohan FM & Perry EB (2007) A systematics for discovering the fundamental units of
464 bacterial diversity. *Curr. Biol* 17: R373-R386.
- 465 de Las Rivas B, Marcobal A & Muñoz R (2006) Development of a multilocus sequence
466 typing method for analysis of *Lactobacillus plantarum* strains. *Microbiology*
467 152:85-93.
- 468 Didelot X & Falush D (2007) Inference of bacterial microevolution using multilocus
469 sequence data. *Genetics* 175: 1251-1266.
- 470 Drake JW (1991) A constant rate of spontaneous mutation in DNA-based microbes.
471 *Proc. Natl. Acad. Sci USA* 88(16): 7160-7164.

472

473

- 1
2
3 474 Drummond LC, Balboa S, Beaz R, Mulcahy MF, Barja JL, Culloty SC & Romalde, J.L.
4 475 (2007) The susceptibility of Irish-grown and Galician-grown Manila clams,
5 476 *Ruditapes philippinarum*, to *Vibrio tapetis* and brown ring disease. *J Invertebr*
6 477 *Pathol* 95: 1-8.
7
8
9 478 Excoffier L & Lischer JEL (2010) Arlequin suite ver 3.5: A new series of programs to
10 479 perform population genetics analyses under Linux and Windows. *Mol Ecol Res* 10:
11 480 564-567.
12
13 481 Feil EJ, Li, BC, Aanensen DM, Hanage WP & Spratt BG (2004) eBURST: inferring
14 482 patterns of evolutionary descent among clusters of related bacterial genotypes from
15 483 multilocus sequence typing data. *J Bacteriol* 186: 1518-1530.
16
17 484 Fu YX (1997) Statistical tests of neutrality of mutations against population growth,
18 485 hitchhiking and background selection. *Genetics* 147: 915–925.
19
20 486 Fu Y-X & Li, W-H (1993) Statistical tests of neutrality of mutations. *Genetics* 133:
21 487 693-709.
22
23 488 Gordon DM, Bauer S & Johnson, JR (2002) The genetic structure of *Escherichia coli*
24 489 populations in primary and secondary habitats. *Microbiology* 148: 1513–1522
25
26 490 Hanage WP, Spratt BG, Turner KM & Fraser C (2006) Modelling bacterial speciation.
27 491 *Philos Trans R Soc Lond B Biol Sci* 361: 2039-2044.
28
29 492 Huson DH & Bryant D (2006) Application of phylogenetic networks in evolutionary
30 493 studies. *Mol Biol Evol* 23:254-267.
31
32 494 Jensen JL, Bohonak AJ & Kelley ST (2005) Isolation by distance, web service. *BMC*
33 495 *Genet* 6: 13.
34
35 496 Jolley KA & Maiden MCJ (2010) BIGSdb: scalable analysis of bacterial genome
36 497 variation at the population level. *BMC Bioinformatics* 11: 595.
37
38 498 Kimura M (1983) *The neutral theory of molecular evolution*. Cambridge University
39 499 Press. Cambridge.
40
41 500 Librado P & Rozas J (2009) DnaSP v5: a software for comprehensive analysis of DNA
42 501 polymorphism data. *Bioinformatics* 25: 1451-1452.
43
44 502 Maiden MC (2006) Multilocus sequence typing of bacteria. *Ann Rev Microbiol* 60: 561-
45 503 588.
46
47 504 Martin DP, Lemey P, Lott M, Moulton V, Posada D & Lefevre, P. (2010) RDP3: a
48 505 flexible and fast computer program for analyzing recombination. *Bioinformatics* 26:
49 506 2462–2463.
50
51
52
53
54
55
56
57
58
59
60

- 1
2
3 507 Maynard-Smith J, Smith NH, O'Rourke M & Spratt BG (1993) How clonal are
4 508 bacteria? *Proc Natl Acad Sci USA* 90: 4384-4388.
- 5
6 509 Nei M (1978) Estimation of average heterozygosity and genetic distance from a small
7 510 number of individuals. *Genetics* 89: 583-590.
- 8
9 511 Nei M & Gojobori T (1986) Simple methods for estimating the numbers of synonymous
10 512 and non synonymous nucleotide substitutions. *Mol Biol Evol* 3: 418-426.
- 11
12 513 Paillard C (2004) A short-review of brown ring disease, a vibriosis affecting clams,
13 514 *Ruditapes philippinarum* and *Ruditapes decussatus*. *Aquat Living Resour* 17: 467-
14 515 475.
- 15
16 516 Pérez-Losada M, Browne EB, Madsen A, Wirht T, Viscidi RP & Crandall KA (2006)
17 517 Population genetics of microbial pathogens estimated from multilocus sequence
18 518 typing (MLST) data. *Infect Genet Evol* 6: 97-112.
- 19
20 519 Ramos-Onsins SE & Rozas J (2002) Statistical properties of new neutrality tests against
21 520 population growth. *Mol Biol Evol* 19: 2092-2100.
- 22
23 521 Ray N, Currat M & Excoffier L (2003) Intra-deme molecular diversity in spatially
24 522 expanding populations. *Mol Biol Evol* 20: 76-86.
- 25
26 523 Rodríguez JM, López-Romalde S, Beaz R, Alonso MC, Castro D & Romalde JL (2006)
27 524 Molecular fingerprinting of *Vibrio tapetis* strains using three PCR-based methods:
28 525 ERIC-PCR, REP-PCR, and RAPD. *Dis Aquat Org* 69: 175-183.
- 29
30 526 Rogers AR & Harpending H (1992) Population growth makes waves in the distribution
31 527 of pairwise genetic differences. *Mol Biol Evol* 9: 552-569.
- 32
33 528 Romalde JL, Magariños B, Villar C, Barja JL & Toranzo AE (1999) Genetic analysis of
34 529 turbot pathogenic *Streptococcus parauberis* strains by ribotyping and random
35 530 amplified polymorphic DNA. *FEMS Microbiol Lett* 179: 297-304.
- 36
37 531 Sikorski J (2008) Populations under microevolutionary scrutiny: what will we gain?
38 532 *Arch Microbiol* 189: 1-5.
- 39
40 533 Slatkin M (1993) Isolation by distance in equilibrium and non equilibrium populations.
41 534 *Evolution* 47: 264-279.
- 42
43 535 Slatkin M & Hudson RR (1991) Pairwise comparisons of mitochondrial DNA
44 536 sequences in stable and exponentially growing populations. *Genetics* 129: 555-62.
- 45
46 537 Smith JM, Smith NH, O'Rourke M & Spratt BG (1993) How clonal are bacteria? *Proc*
47 538 *Natl Acad Sci USA* 90:4384-4388.
- 48
49
50
51
52
53
54
55
56
57
58
59
60

- 1
2
3 539 Städler T, Haubold B, Merino C, Stephan W & Pfaffelhuber P (2009) The impact of
4 sampling schemes on the site frequency spectrum in subdivided populations.
5
6 540 *Genetics* 182: 205-216.
7
8 541
9 542 Strobeck C (1987) Average number of nucleotide differences in a simple from a single
10 543 subpopulation: a test for population subdivision. *Genetics* 117: 149-153.
11 544 Tajima F (1989) Statistical method for testing the neutral mutation hypothesis by DNA
12 545 polymorphisms. *Genetics* 123: 585-595.
13 546 Tamura K, Peterson D, Peterson N, Stecher G, Nei M & Kumar S (2011) MEGA5:
14 547 Molecular evolutionary genetics analysis using Maximum Likelihood, evolutionary
15 548 distance, and Maximum Parsimony methods. *Mol Biol Evol* 28: 2731-2739.
16 549 Tanabe Y & Watanabe MM (2011) Local Expansion of a Panmictic Lineage of Water
17 550 Bloom-Forming Cyanobacterium *Microcystis aeruginosa* *PLoS One* 6(2): e17085.
18 551 Urwin R & Maiden MC (2003) Multilocus sequence typing: a tool for global
19 552 epidemiology. *Trends Microbiol* 11: 479-87.
20 553 Wright S (1951) The genetical structure of populations. *Annals of Eugenics* 15: 323-
21 554 354.
22 555 Yan Y, Cui Y, Han H, Xiao X, Won HC, Tan Y, Guo Z, Liu X, Yang R & Zhou D
23 556 (2011) Extended MLST-based population genetics and phylogeny of *Vibrio*
24 557 *parahaemolyticus* with high levels of recombination. *Int J Food Microbiol* 145:106-
25 558 12.
26 559
27 560
28 561
29 562
30 563
31 564
32 565
33 566
34 567
35 568
36 569
37 570
38 571
39 572
40
41
42
43
44
45
46
47
48
49
50
51
52
53
54
55
56
57
58
59
60

573

574

Figure legends

575

576 **Fig. 1.** Median Joining network based on the concatenated sequence of the 10
577 housekeeping genes. Size of the circle are proportional to the size of each ST. Next
578 to each circle are shown the strains belonging to each ST. Color of the circles
579 indicates the country origin of the isolates. Open circles represent putative
580 intermediated sequences. Numbers indicates nucleotidic substitutions.

581 **Fig. 2.** Neighbor-Net graph based on the concatenated sequence of the 10 housekeeping
582 genes of the 30 isolates of *V. tapetis* showing a bushy network structure indicative of
583 pervasive recombination.

584 **Fig. 3.** Clonal genealogy (A) and evolutionary events on each node (B) reconstructed
585 following the majority rule from the concatenated sequence. The designations for the
586 nodes (A-L) in part (A) are congruent with the designations of rows in part (B). Each
587 column in part B delineates the extent of each gene constituting the concatenated.
588 The height of the red line indicates the probability of recombination on a scale from
589 0 (row bottom) to 1 (row top). Each nucleotide substitution is represented by a black
590 cross.

591 **Fig. 4.** Mismatch distribution of the whole population of *V. tapetis*. Bars indicates
592 observed frequency of each pairwise difference. The line graphs correspond to the
593 expected distribution of the mismatches following four different population
594 expansion models.

595 **Fig. 5.** Moran's correlogram of individual allele frequencies. Moran's I , and index of
596 spatial autorrelation was plotted for individual allele frequencies across 4 qually
597 sized distances.

598

599

600

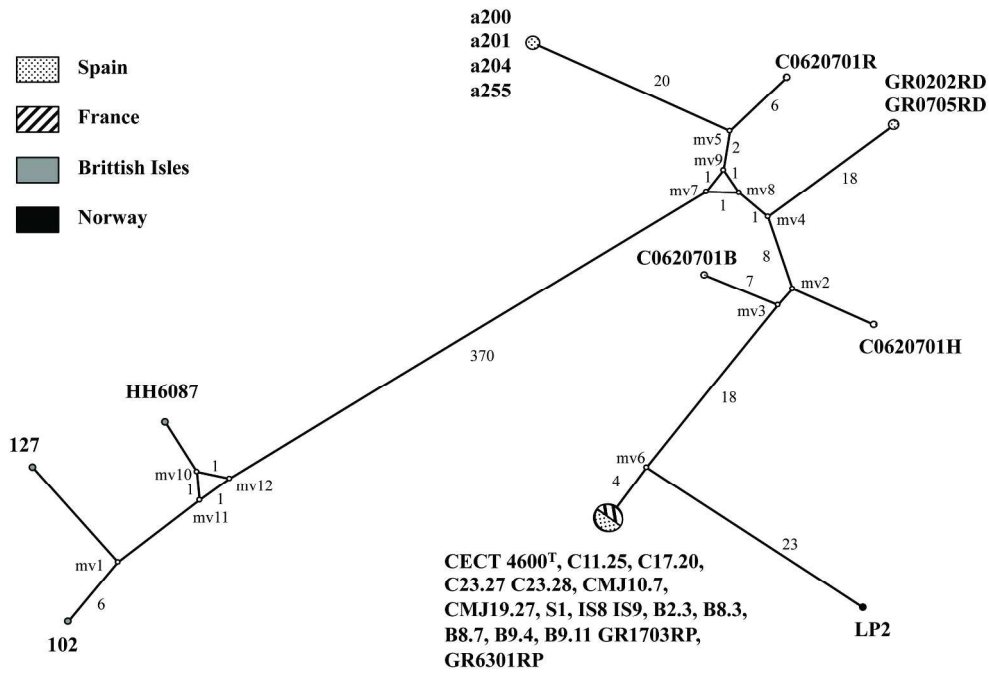
601

602

603

604

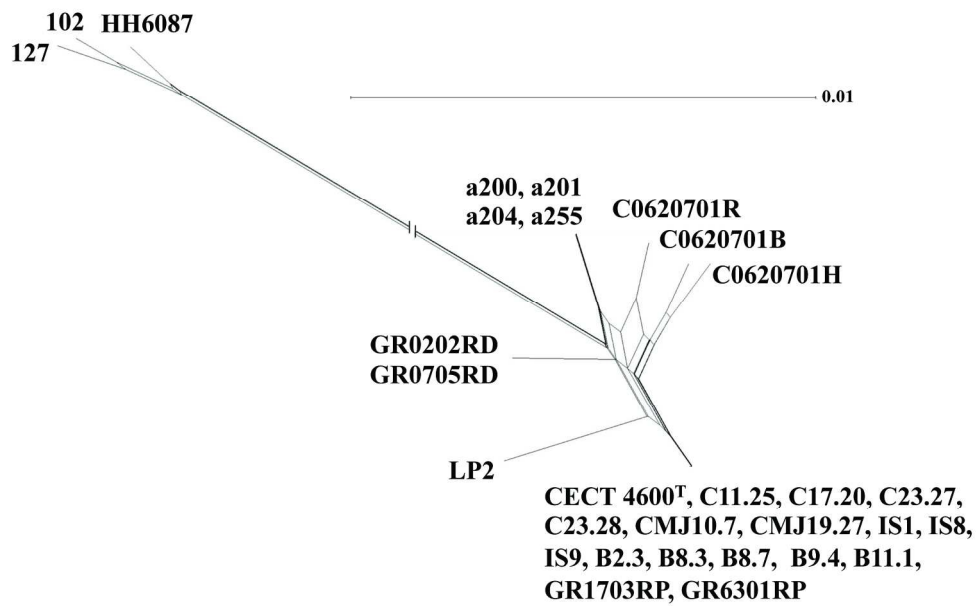
605



Median Joining network based on the concatenated sequence of the 10 housekeeping genes. Size of the circle are proportional to the size of each ST. Next to each circle are shown the strains belonging to each ST. Color of the circles indicates the country origin of the isolates. Open circles represent putative intermediated sequences. Numbers indicates nucleotidic substitutions.

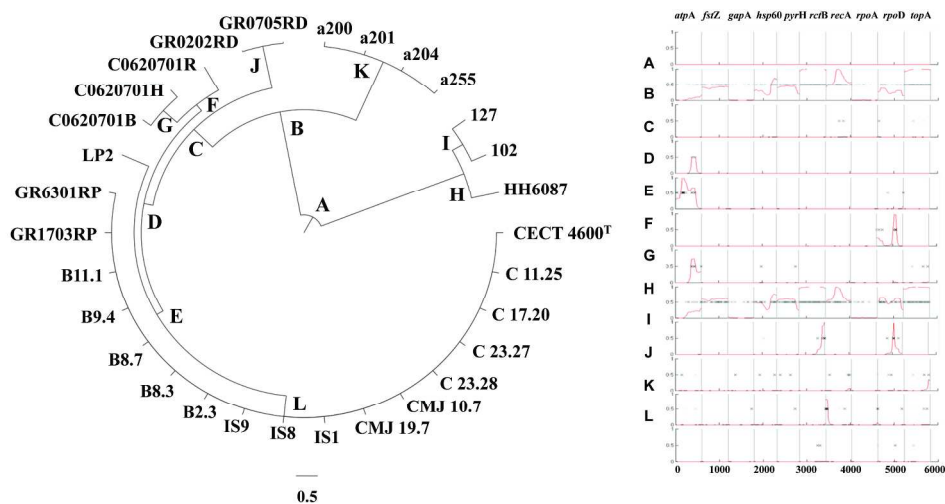
239x163mm (300 x 300 DPI)

1
2
3
4
5
6
7
8
9
10
11
12
13
14
15
16
17
18
19
20
21
22
23
24
25
26
27
28
29
30
31
32
33
34
35
36
37
38
39
40
41
42
43
44
45
46
47
48
49
50
51
52
53
54
55
56
57
58
59
60

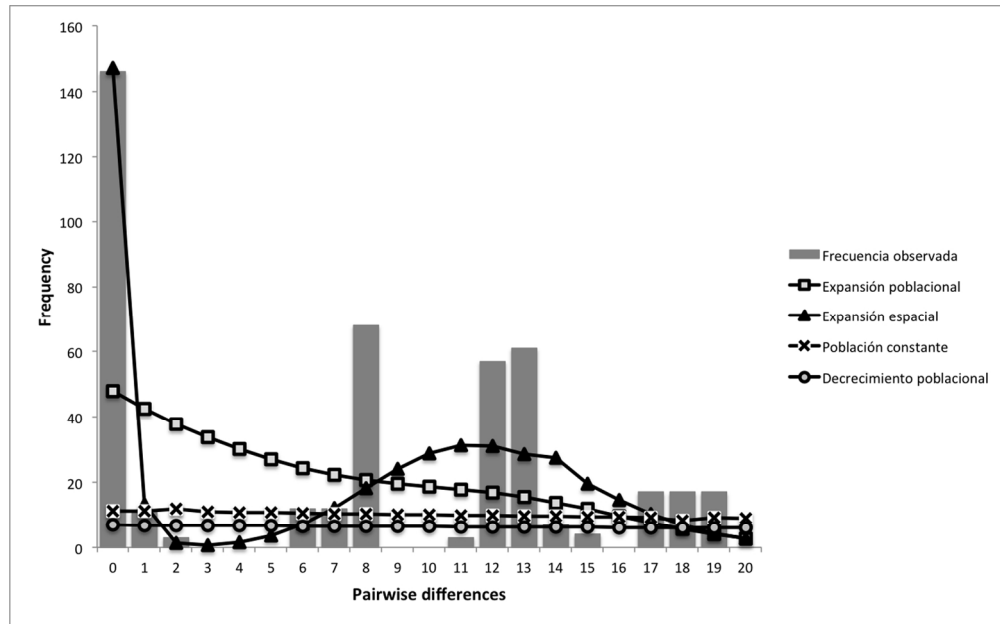


Neighbor-Net graph based on the concatenated sequence of the 10 housekeeping genes of the 30 isolates of *V. tapetis* showing a bushy network structure indicative of pervasive recombination.
189x116mm (300 x 300 DPI)

Review



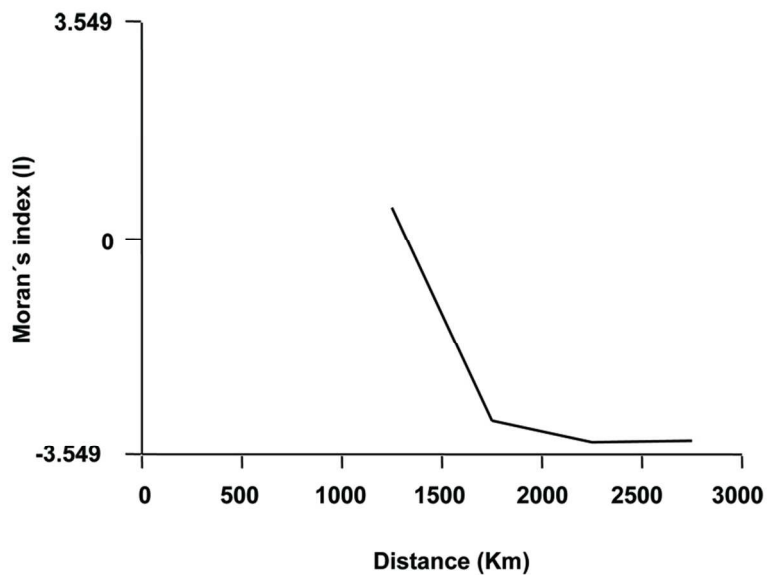
. Clonal genealogy (A) and evolutionary events on each node (B) reconstructed following the majority rule from the concatenated sequence. The designations for the nodes (A-L) in part (A) are congruent with the designations of rows in part (B). Each column in part B delineates the extent of each gene constituting the concatenated. The height of the red line indicates the probability of recombination on a scale from 0 (row bottom) to 1 (row top). Each nucleotide substitution is represented by a black cross.
235x125mm (300 x 300 DPI)



Mismatch distribution of the whole population of *V. tapetis*. Bars indicates observed frequency of each pairwise difference. The line graphs correspond to the expected distribution of the mismatches following four different population expansion models.
150x93mm (300 x 300 DPI)

Review

1
2
3
4
5
6
7
8
9
10
11
12
13
14
15
16
17
18
19
20
21
22
23
24
25
26
27
28
29
30
31
32
33
34
35
36
37
38
39
40
41
42
43
44
45
46
47
48
49
50
51
52
53
54
55
56
57
58
59
60



Moran's correlogram of individual allele frequencies. Moran's I, and index of spatial autorrelation was plotted for individual allele frequencies across 4 equally sized distances.
99x82mm (300 x 300 DPI)

view

1
2
3
4
5
6
7
8
9
10
11
12
13
14
15
16
17
18
19
20
21
22
23
24
25
26
27
28
29
30
31
32
33
34
35
36
37
38
39
40
41
42
43
44
45
46
47
48
49
50
51
52
53
54
55
56
57
58
59
60

**Disentangling the structure and evolution of the population of the clam pathogen
Vibrio tapetis.**

Sabela Balboa, Asmine Bastardo, Jesús L. Romalde

Supplementary Material

For Peer Review

Table S1: Average number of nucleotide differences per site for two randomly selected strains (π) and average number of nucleotide differences per site (θ) for each individual gene and the concatenated sequence in each subspecies

Gene	<i>V. tapetis</i> subsp. <i>tapetis</i>		<i>V. tapetis</i> subsp. <i>britannicus</i>	
	π	θ	π	θ
<i>atpA</i>	0.00752	0.00679	0.00089	0.00073
<i>fstZ</i>	0.00093	0.00123	0.00349	0.00286
<i>gapA</i>	0.00120	0.00171	0	0
<i>hsp60</i>	0.00150	0.00346	0.00203	0.00167
<i>pyrH</i>	0.00314	0.00396	0.00310	0.00255
<i>rctB</i>	0,00242	0,00259	0,00622	0,00511
<i>recA</i>	0.00646	0.00711	0.00265	0.00218
<i>rpoA</i>	0.00034	0.00049	0	0
<i>rpoD</i>	0.00930	0.00850	0.00486	0.00399
<i>topA</i>	0.00715	0.00735	0.00240	0.00197
MLSA	0.00523	0.00547	0.00200	0.00165

Table S2: Summary statistics of demographic history of the subspecies *V. tapetis* subsp. *tapetis*

Gene	D	D*	F*	F _S	S	R ₂
<i>atpA</i>	0.608	0.772	0.810	1.462	0.506	0,203
<i>fstZ</i>	-1.132	-1.155	-1.195	-0.858	0.934	0,236
<i>gapA</i>	-1.358	-1.427	-1.522	-1.798	0.974	0,165
<i>hsp60</i>	-1.719	-1.435	-1.768	-1.377	0.927	0,091
<i>pyrH</i>	-1.024	-0.969	-1.066	-2.019	0.980	0,153
<i>rctB</i>	-0.195	-1.046	-0.925	0.241	0.688	0,123
<i>recA</i>	-0.504	-0.318	-0.396	-2.920	1.000	0,147
<i>rpoA</i>	-1.006	-1.049	-1.101	-0.095	0.890	0,350
<i>rpoD</i>	0.520	0.341	0.420	-2.208	1.000	0,350
<i>topA</i>	-0.151	-0.354	-0.339	-1.228	0.958	0,177
MLSA	-0.247	-0.258	-0.283	0.163	1.000	0,165

Note: D, Tajima's D statistic (Tajima, 1989); D* and F*, Fu and Li statistics (Fu and Li, 1993); F_S, Fu's statistic (Fu, 1997); S', Strobeck's statistic (Strobeck, 1987); R₂, Onsis R₂ statistic (Ramos-Onsins and Rozas, 2002)

Figure S1. Population structure of *V. tapetis*. (A) Population snapshot of all the sequence types (ST) of the MLST using eBurst program. The sizes of the circle are related to the number of strains within each ST. (B) Dot graph base don majority rule consensus tree. Ancestral nodes are showed in black and the location of isolates in red, with each red line indicating a single isolate. The empty circles indicate putative ancestral nodes

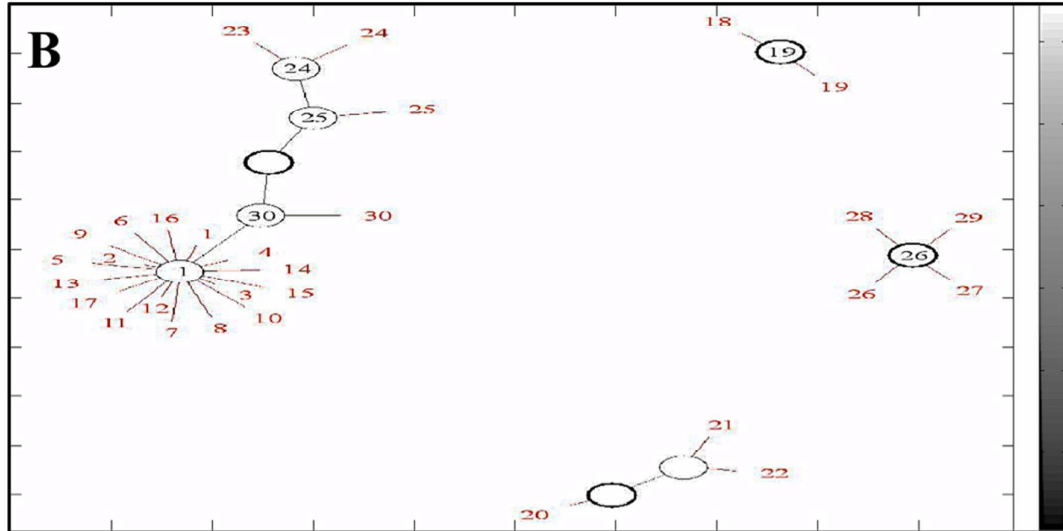
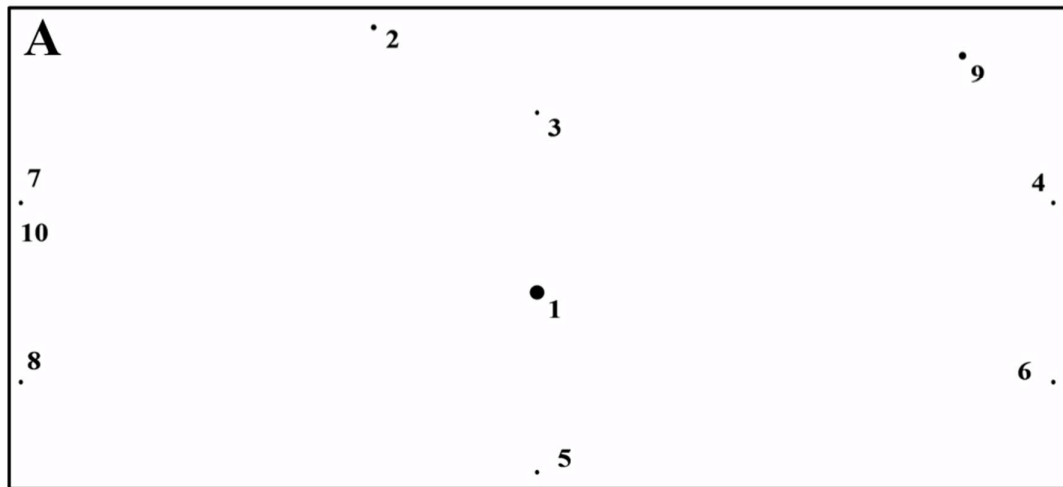


Figure S2. Phylogenetic reconstruction based on the concatenation of nucleotide sequences using the 30 isolates of *V. tapetis*. by Neighbor Joining algorithm. Bar, expected nucleotide substitutions per site. Only bootstrap values above 70% are shown (1000 resamplings) at each branch point.

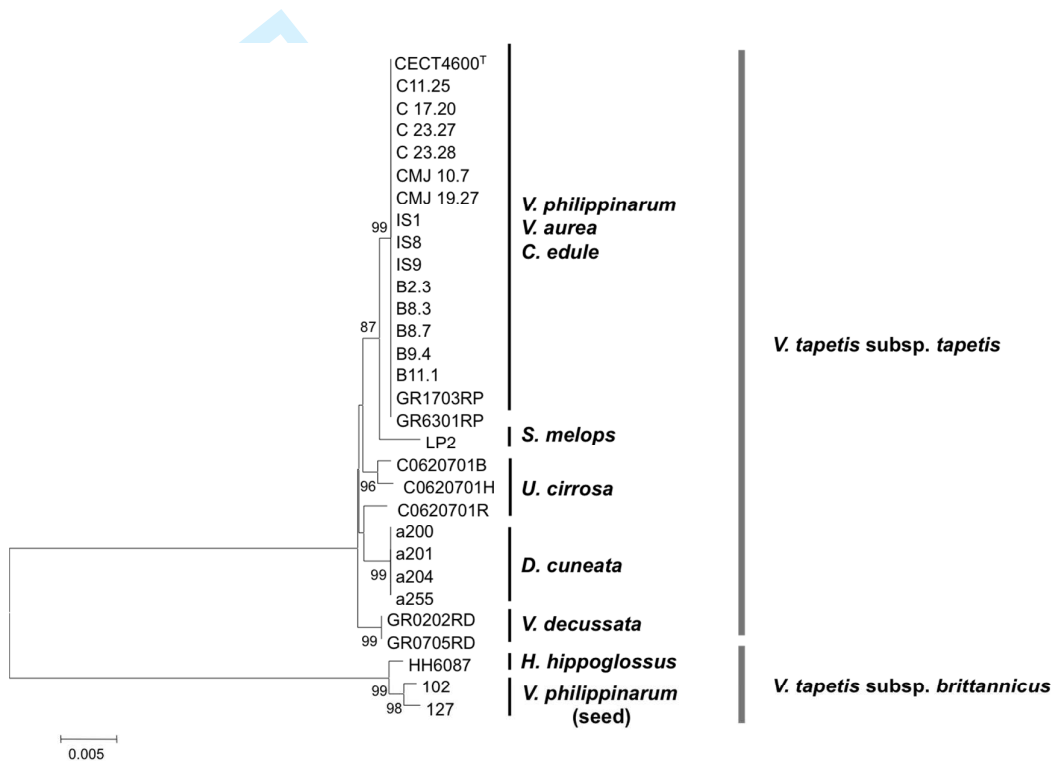
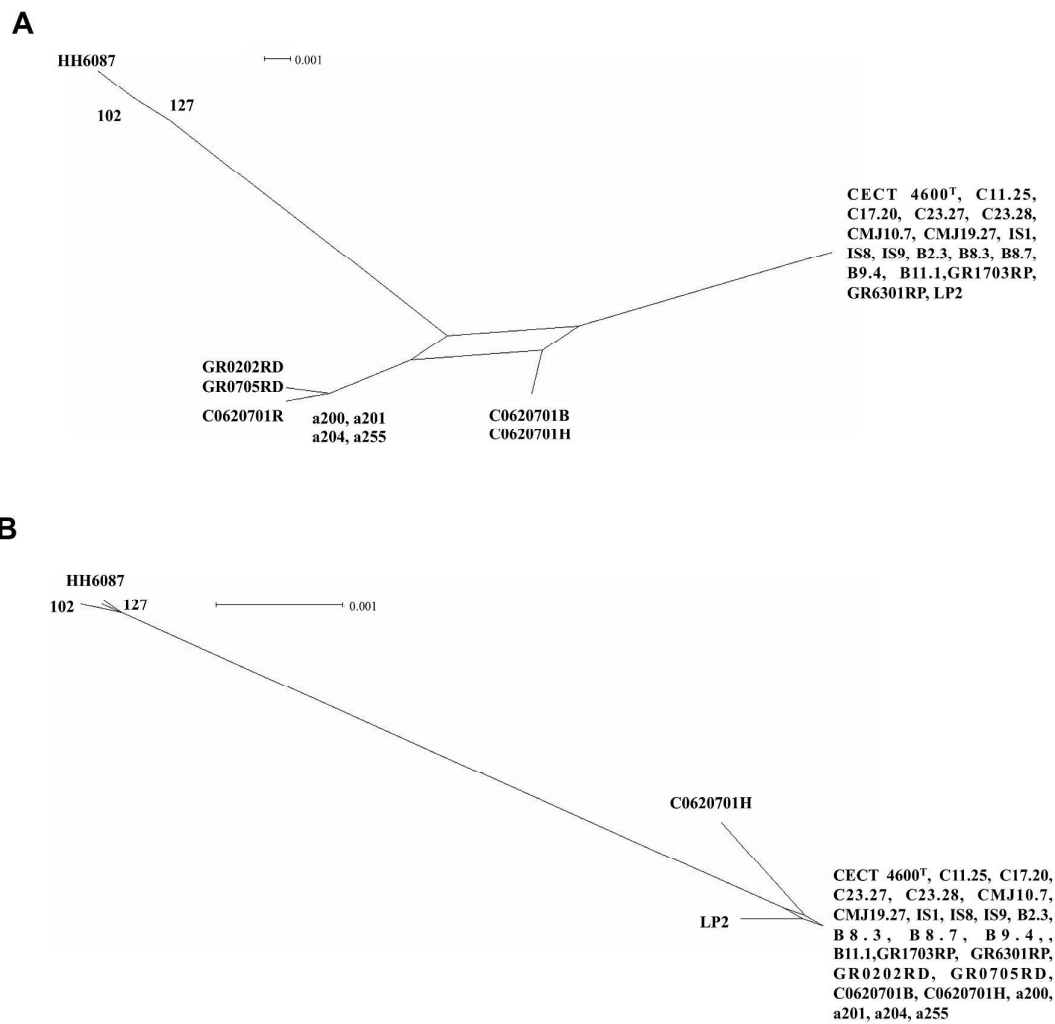
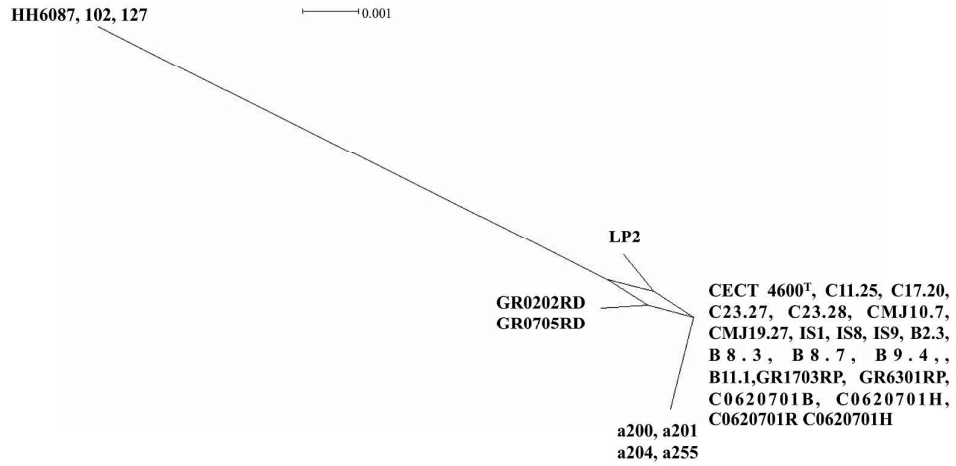


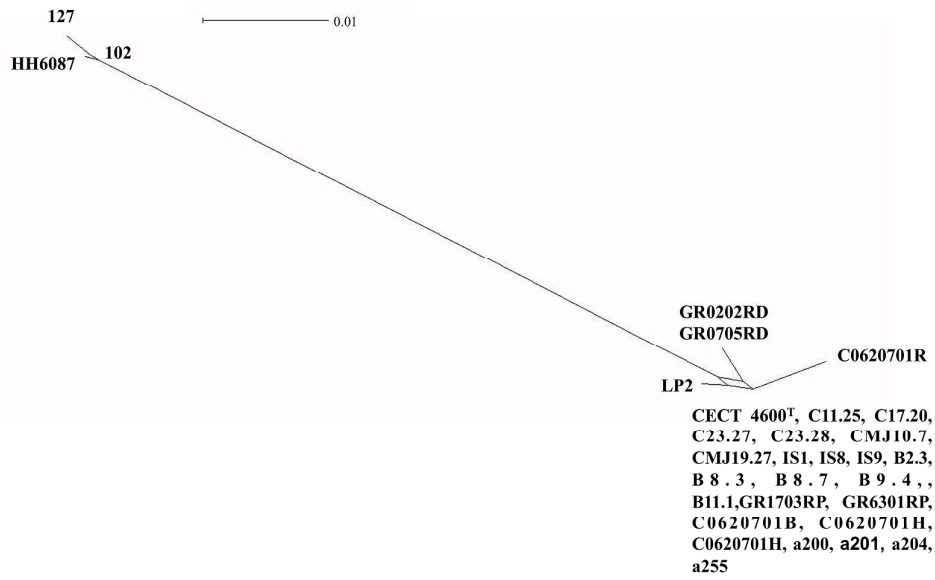
Figure S3. Neighbor-Net graph based on the individual housekeeping genes of the 30 isolates of *V. tapetis*. A, *atpA*; B, *fstZ*; C, *pyrH*; D, *rctB*; E, *recA*; F, *rpoD*.



C

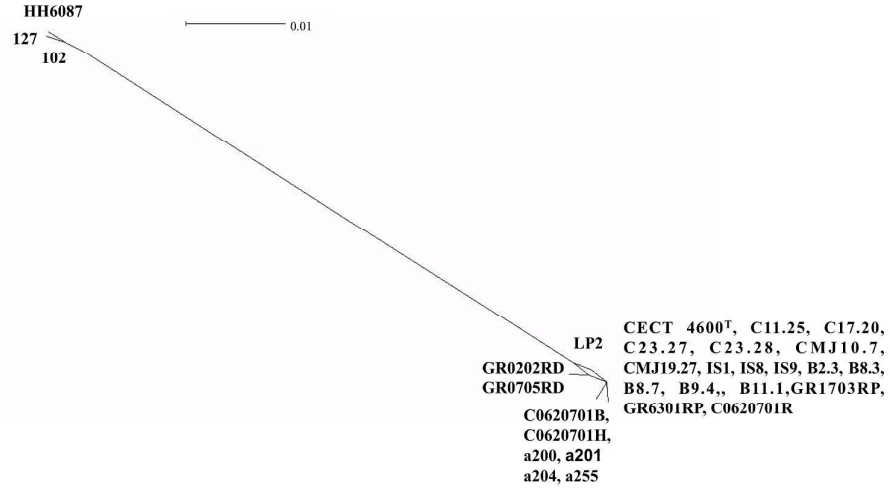


D

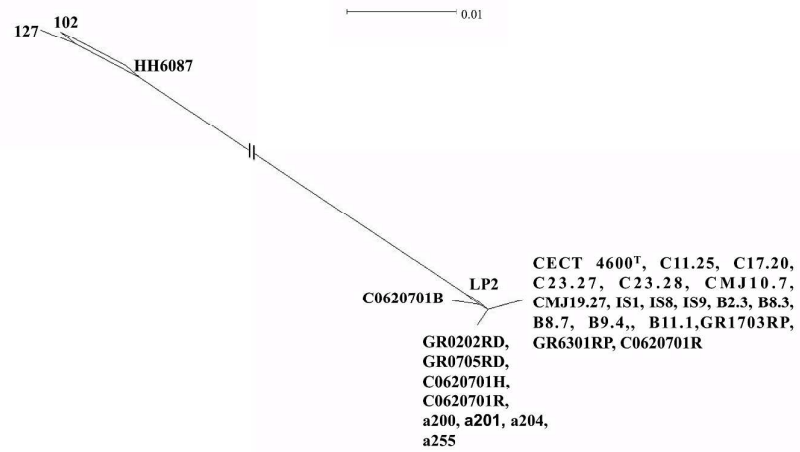


1
2
3
4
5
6
7
8
9
10
11
12
13
14
15
16
17
18
19
20
21
22
23
24
25
26
27
28
29
30
31
32
33
34
35
36
37
38
39
40
41
42
43
44
45
46
47
48
49
50
51
52
53
54
55
56
57
58
59
60

E



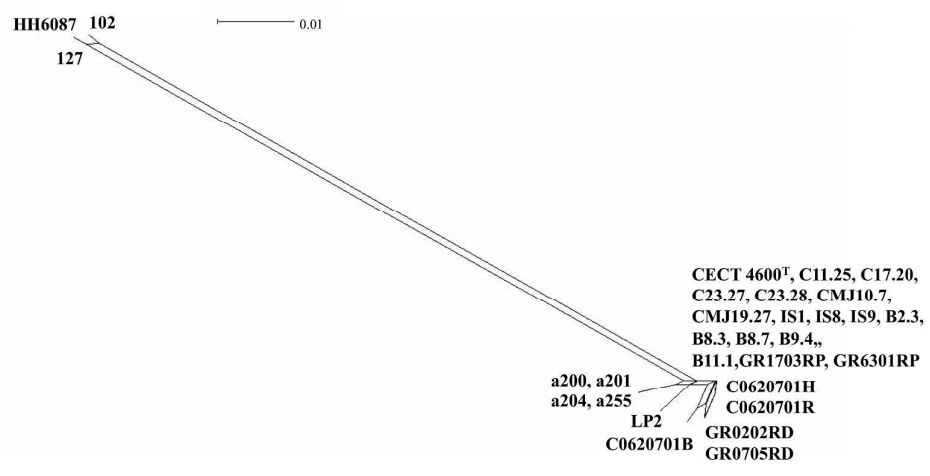
F



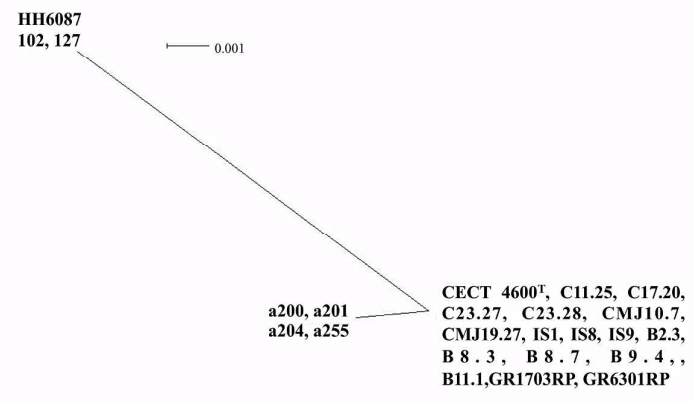
ew

1
2
3
4
5
6
7
8
9
10
11
12
13
14
15
16
17
18
19
20
21
22
23
24
25
26
27
28
29
30
31
32
33
34
35
36
37
38
39
40
41
42
43
44
45
46
47
48
49
50
51
52
53
54
55
56
57
58
59
60

G

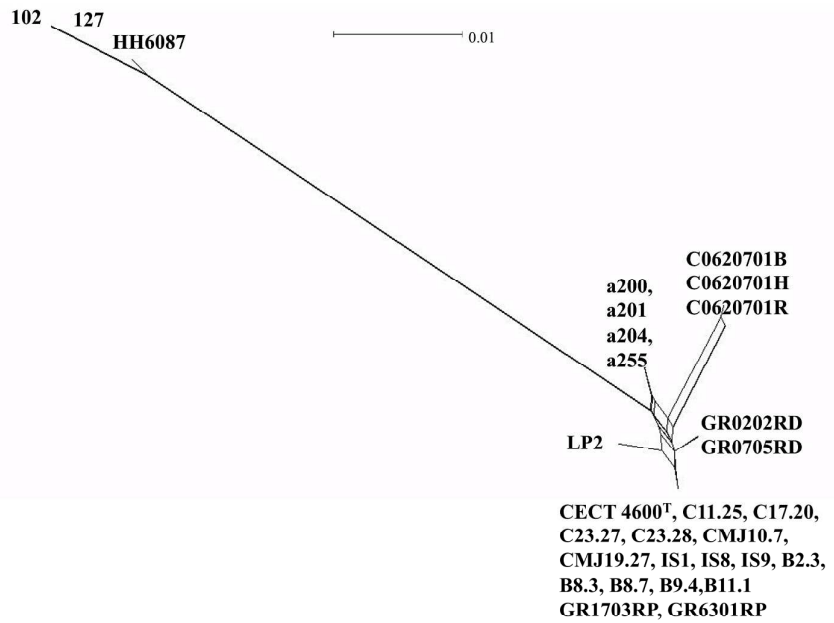


H



1
2
3
4
5
6
7
8
9
10
11
12
13
14
15
16
17
18
19
20
21
22
23
24
25
26
27
28
29
30
31
32
33
34
35
36
37
38
39
40
41
42
43
44
45
46
47
48
49
50
51
52
53
54
55
56
57
58
59
60

I



J

